MIC2023
23rd Machining Innovations Conference for Aerospace Industry

Proceedings are available on SSRN: www.ssrn.com

SSRN Proceedings Hosted on SSRN.com

MIC Procedia (2023) 025–032

23rd Machining Innovations Conference for Aerospace Industry 2023 (MIC 2023), 29th and 30th November 2023, Hannover, Germany

Efficient Cutting Fluid Supply in Additively Manufactured Indexable Helical Milling Tools for Roughing of Ti-6Al-4V

T.Kelliger[a,*], M.Meurer[a], T. Bergs[a,b]

[a]*Laboratory for Machine Tools and Production Engineering (WZL) of RWTH Aachen University, Campus-Boulevard 30, 52074 Aachen, Germany*
[b]*Fraunhofer Institute for Production Technology (IPT), Steinbachstr. 17, 52074 Aachen, Germany*

* Corresponding author. Tel.: +49 241 80-20523. *E-mail address:* t.kelliger@wzl.rwth-aachen.de

Abstract

High-pressure cutting fluid supply in milling allows higher productivities and results in longer tool life and higher process reliability. By using the additive manufacturing (AM) technique of Laser Powder Bed Fusion (PBF-LB), steel-based basic bodies for indexable cutting tools can be manufactured including complex internal structures with very few geometrical limitations. Thus, the internal cutting fluid supply can be redesigned, lowering fluid losses within the supply channels and focusing the fluid for a more efficient and effective cooling and lubrication of the contact zone between tool and workpiece. In this study, a focused and low-loss fluid supply in a 16-edged, four-row indexable helical milling tool was developed with support of CFD simulations. The tool was then PBF-LB manufactured with a low-alloyed case hardening steel 18MnCrMoV4-8-7, post-processed by the tool manufacturer and applied in a roughing operation for the manufacturing of an airplane structural component made from aerospace-alloy Ti-6Al-4V. Extensive machining experiments were conducted comparing additively and conventionally manufactured tools of the same geometry. The analysis of tool wear, chip form and process torque showed the operational readiness and potential of AM cutting tools for industrial purposes even in challenging and heavy duty machining conditions.

Keywords: Milling; Additive Manufacturing, PBF-LB, Ti-6Al-4V, Cutting Fluid Supply; Bainidur AM

1. Introduction

Internal, often high-pressure cutting fluid (CF) supply is crucial in productive milling operations of difficult-to-cut materials used e.g. in aerospace applications [1,2]. CF assisted machining demands high power consumptions with the high-pressure unit making up more than 20 % of the total power use in some machine tools [3]. Therefore, an efficient use of CF is essential regarding the goal of a sustainable and emission-friendly production process.

Investigations by Lakner et al. proved the potential of an adapted, workpiece material dependent internal CF supply at a supply pressure of p = 80 bar [4]. With an adapted orientation of the outlet nozzle, the CF free jet was directed on the rake face, leading to significant improvements in tool life during roughing of Ti-6Al-4V and AISI4140+QT. However, the design of an individually adapted CF supply with conventional manufacturing techniques is complex, expensive and limited in terms of geometrical freedom of design. Additive manufacturing (AM) techniques such as Laser Powder Bed Fusion (PBF-LB) offer extended possibilities of manufacturing cutting tools with complex external and internal geometrical features [5]. Examples of indexable AM cutting tools can be found in research as well as in industrial application. Scientific examples range from topology optimization to an improvement in damping behavior and an adjustment of the CF supply

[2,6-8]. First industry-proven AM cutting tools are offered by different tool manufacturers for drilling, groove-turning and milling operations [9-11]. Lakner et al. tested a PBF-LB manufactured single-row indexable tangential milling tool made from tool steel 1.2709 with an adapted CF supply. In roughing of 42CrMo4+QT, the tool life could be improved by 67 % compared to the conventionally manufactured reference tool [12]. In roughing of Ti-6Al-4V with a similar AM tool, containing a CF supply specifically designed for this workpiece material, no improvements regarding tool life were observed [13].

Even though the general potentials of PBF-LB manufactured indexable milling tools with adapted CF supply have been demonstrated, operators and users have so far been reluctant to use AM tools in an industrial environment. Especially for heavy duty machining, the possibilities of AM tools have not been investigated.

In this study, a 16-edged, four-row indexable helical milling tool was redesigned according to previous findings presented in [14-16] regarding an adapted, low-loss and targeted cutting fluid supply, additively manufactured in PBF-LB and evaluated in roughing of Ti-6Al-4V in machining experiments. The goal was to prove the potential and operational readiness of PBF-LB manufactured cutting tools in an industrial and challenging environment. Three tools were investigated: a conventionally manufactured reference tool with standard CF supply, an AM tool with standard CF supply and an AM tool with adapted CF supply. In the following, the redesigned channel and nozzle characteristics are presented, the underlying ideas for a reliable post-processing of the PBF-LB as-built raw bodies discussed and the results of the machining experiments given.

2. Redesign of an efficient cutting fluid supply

The design process focused on the CF supply and thus on the channel and nozzle geometries only. Therefore, the macro-geometry of the basic body was not changed. In consultation with the involved tool manufacturer Walter AG, a standard catalogue tool for cutting of titanium alloys was chosen as reference tool. The tangential helical milling tool Walter Tools F5138.B27.063.Z04.45 has 16 insert seats in total, with four rows of four inserts each, a diameter of D = 63 mm and a total length of l = 70 mm. The tool is mounted on a tool holder with a mounting diameter of 27 mm according to DIN 8030 [17].

2.1. Analysis of reference cutting fluid supply

The cutting fluid is supplied through the spindle and exits the tool holder on the front side through four channels (channel diameter d = 3.4 mm). Each insert is supplied with a coolant stream via a straight channel (drilled, diameter d = 2.5 mm) from the main filled space between tool holder and tool. The channel layout is shown in Fig. 1. For the supply of the upper three rows, the fluid has to flow through the gap between mounting screw and tool. The position and angle of incidence of the outlet does not allow a focused and concentrated fluid supply towards the highly stressed cutting edge. The position and incidence angle differ between each row and do not seem to follow any regularity but are rather defined by the manufacturability. As the cross section is not reduced towards the outlet, the fluid is not accelerated and exits the channel without any increase in kinetic energy. Fig. 1 additionally shows the numbering of the row and insert used throughout the whole investigation.

The analysis reveals the potential for a reduction of pressure losses due to turbulences and abrupt change of flow direction as well as for a more focused CF free jet with high local fluid velocity directed directly on the cutting edge.

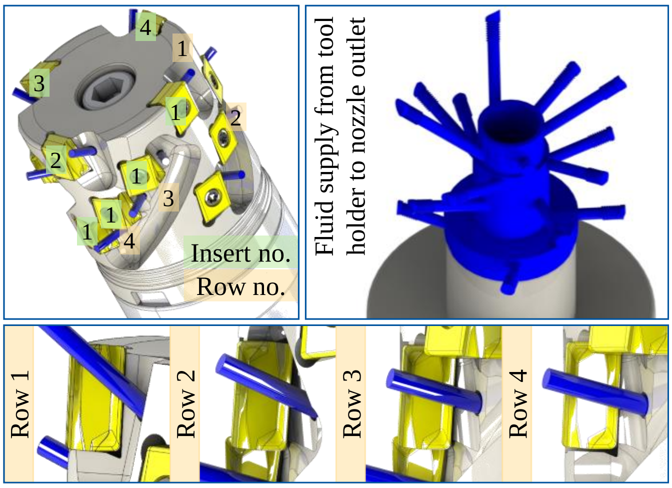

Fig. 1. Cutting fluid supply in the conventional reference tool and numeration of rows and inserts

2.2. Development of adapted channel and nozzle characteristic in the AM tool

As stated above, the tool geometry of the AM tool was not changed compared to the reference tool. The technical redesign of the CF supply aimed to optimize the tool performance for roughing of Ti-6Al-4V. Therefore, previous findings regarding a favorable nozzle geometry, free jet impact point and angle of incidence, taking into account the geometrical freedom of the PBF-LB process, were included. These investigations showed an improvement of tool life along with a decrease of volume flow for roughing of Ti-6Al-4V when focusing the CF on the rake face at a small distance from the cutting edge. With a small incidence angle between free jet and rake face, the fluid can penetrate deep into the gap between chip and rake face, maximizing the cooling effect and affecting the chip curling. Furthermore, the jet formation can be influenced by an adapted nozzle design, wetting only the heat-stressed area of the cutting insert. Splitting up the volume flow to several outlet nozzles helps to accelerate the fluid locally, improving the cooling capability as well as the mechanical effect of the free jet. Initial results can be found in [16].

The derived nozzle design for the AM tool with adapted CF supply AM_{CF} is displayed in Fig. 2. The CF supply was individually adapted for each row according to the geometric boundary conditions. Following nozzle geometries were applied:

- Row 1: L-formed and elliptical nozzles directed towards the corner and the center of the cutting edge (distribution of total volume flow 2-1)
- Row 2 & 3: Three elliptical nozzles with the same cross section, wetting the whole length of the cutting edge
- Row 4: One elliptical nozzle directed towards the upper center of the cutting edge

In Fig. 2 the position coordinates (x_{rf}, y_{rf}) and angles of incidence (φ_x, φ_z) which define the ideal fluid jet impingement on the simplified rake face are introduced. All free jets are directed on the rake face at a small distance (y_{rf} = 1.25 mm) from the cutting edge. The total cross-sectional area per insert is comparable for all four rows, leading to similar volume flows in each row (total cross sectional area per insert in CAD model: A_{Outlet} = 3.54 to 3.78 mm^2). As the insert of the first row performs a face-milling operation, it is especially stressed in the corner. Thus, cooling is specifically required in this area. When exploiting the full depth of cut, the inserts in row two and three are fully engaged in peripheral milling. Therefore, the whole length of the cutting edge needs to be cooled. In the fourth row, in most operations only the upper part of the insert is engaged, requiring fluid supply especially in the upper part of the insert. The angle of incidence differs between φ_x = 35° and 60°.

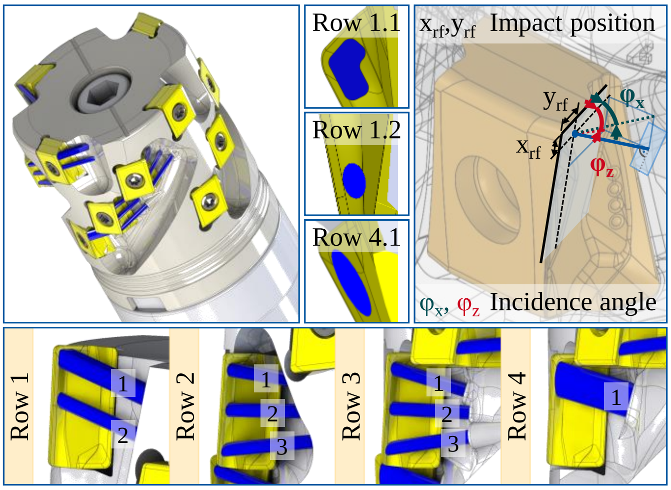

Fig. 2. Derived outlet nozzle design and fluid free jet in the AM_{CF} tool and definition of impact point and incidence angle on simplified rake face

Fig. 3 shows the channel design of the AM_{CF} tool. Contrary to the reference tool, the channel inlets are all located in the cavity between tool holder and tool body only. Each channel supplies two inserts in two different rows, leading to a total number of eight supply channels. The inlet is equipped with a smooth radius. Sharp changes in direction are avoided and the whole channel is designed with smooth transitions for the change of shape between circular channel and geometrically adapted nozzle. The distribution between single inlet channel and several outlet nozzles is designed sharp-edged to reduce flow separations and stagnation zones. In order to guarantee a constant fluid flow, the channel inlet with a diameter of d = 3.25 mm has a bigger cross-sectional area than the maximum total outlet cross-sectional area of all nozzles connected to the supply channel ($A_{channel}$ = 8.3 mm^2 vs. A_{outlet} = 7.4 mm^2).

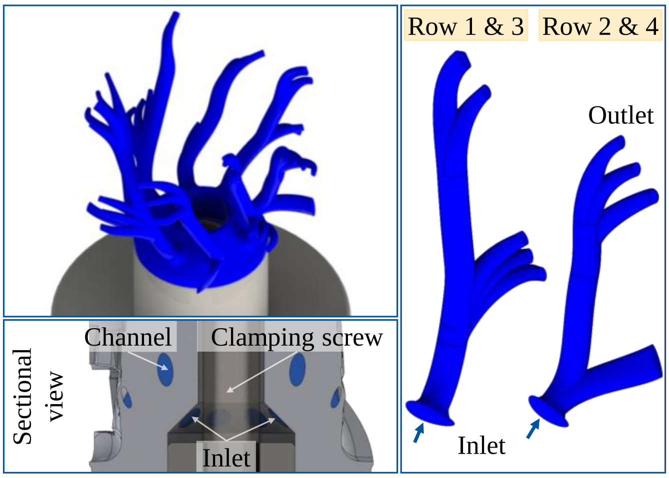

Fig. 3. Channel design in the AM_{CF} tool

The fluid flow characteristics in the supply system were analyzed by means of CFD simulation by utilizing Ansys Fluent, see Fig. 4. The streamlines indicate a low tendency towards flow turbulences and cavitation phenomena due to the smooth channel path. The velocity profiles at the nozzle outlet show homogenous velocity distributions and evenly vectored orientations. The calculated volume flow per outlet nozzle Q at different inlet pressure p is strongly associated with the nozzle cross-sectional area. All nozzles exhibited comparable mean fluid velocities at the outlet (v(p = 30 bar) ≈ 60 m/s; v(p = 70 bar) ≈ 95 m/s). The theoretical volume flow taking into account all 16 insert seats of the tool was reduced by 25 % compared to the reference fluid supply. This can have a significant positive effect on the power consumption of the high-pressure unit [3].

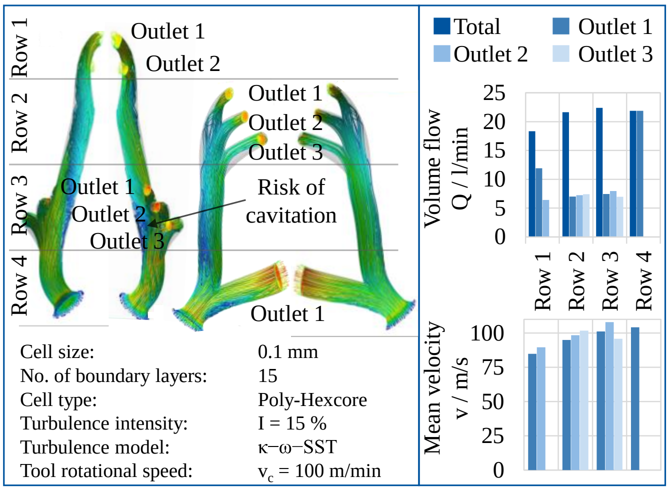

Fig. 4. CFD simulation of the AM_{CF} channels at supply pressure p = 70 bar

3. PBF-LB Manufacturing and post-processing

Three tools were additively manufactured. Two tools included an adapted CF supply whereas the third tool was built without any channels and nozzles. This third tool was post-processed including the reference CF supply. For the machining investigations, only one AM tool with adapted CF supply AM_{CF} and one AM tool with reference CF supply AM_{Ref} were used. All tools were built in one build job on an Aconity Midi PBF-LB machine at Fraunhofer Institute for Laser Technology ILT, Germany. The powder material used was a newly developed low-alloyed case-hardening steel "Bainidur AM", 18MnCrMoV4-8-7, provided by Deutsche Edelstahlwerke Specialty Steel GmbH & Co. KG, which favors the formation of a bainitic microstructure during PBF-LB [18]. A detailed analysis of the microstructure was performed by Bartels et al. [19]. The suitability of the PBF-LB material for indexable milling tools was investigated by Kelliger et al. [15]. The applied process parameters are given in Table 1. Furthermore, adapted downskin and contour parameters developed at ILT were applied to reduce surface roughness and improve accuracy. The total build time of the three tools on one build plate was 24.5 h with a total power consumption of 48.96 kWh. No subsequent heat treatment was conducted.

Table 1. PBF-LB process parameters of the hatch region

Laser power P_L / W	350
Hatch distance Δy_s / µm	100
Layer thickness D_s / µm	60
Scan speed v_s / mm/s	1000
Pre-heating temperature T / °C	200

For post-processing, different features and oversize areas were defined in discussion with the tool manufacturer, see Fig. 5. All insert seats were semi-closed with oversize and angles so that additional support structures could be avoided. The boreholes were closed and oversize added to the fitting and the bottom surface. Referencing of the insert position relative to the fluid supply system was guaranteed by referencing elements on the top and bottom surface of the tool. Post-processing including milling, turning, drilling, tapping and grinding operations was conducted by the tool manufacturer Walter AG in two clamping settings, using the inlet surface of the fluid supply for machining of the mounting as well as the top screw for clamping to the tool holder. No support structures were needed in the interior of the tool. Chip spaces and fluid channels did not undergo any subsequent post-processing.

Results for run-out and surface hardness measured on the backside (measurement device Zwick Roell ZHU) are given in Table 2. The values were comparable between conventional reference tool *Ref* and AM tools with reference CF supply AM_{Ref} and adapted CF supply AM_{CF}.

Table 2. Run-out and macro-hardness of all investigated tools

Tool	Radial run-out / µm	Axial run-out / µm	Hardness / HV30
Reference *Ref*	24	6	448.5
AM Standard fluid supply AM_{Ref}	53	10	445
AM Adapted fluid supply AM_{CF}	28	6	445

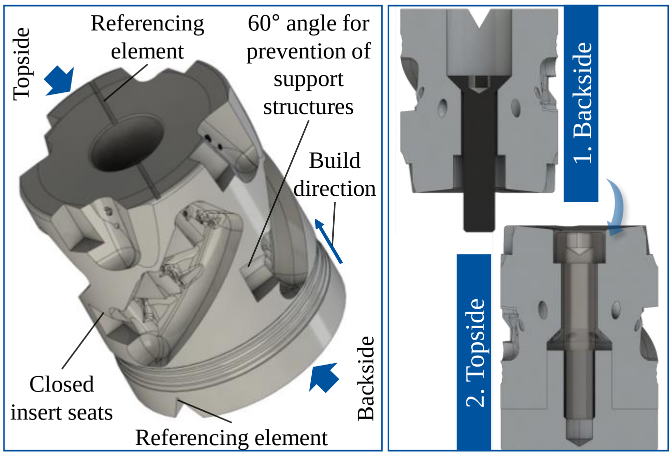

Fig. 5. As-built PBF-LB tool and clamping positions for post-processing

The deviations between the ideal CAD geometry and the post-processed real AM tools were analyzed by optical 3D scanning measurements on a ZEISS Comet 8M in combination with the software GOM Suite. Fig. 6 shows the deviation between CAD and measured geometry for the tools AM_{Ref} and AM_{CF}. The results indicate that a repeatable referencing of the AM blank for post-processing was not reliable with the included referencing elements. Even though the outer contour showed some deviations such as a slight displacement in the axis of rotation, the position of the machined insert seats relative to each other as well as relative to the nozzle positions exhibited high accuracy. This can be explained by the steps of post-processing, where the reference for all machining operations is set at first. The 3D scan was performed before and after the machining experiments to exclude possible influences of plastic deformations caused by high mechanical loads. No changes could be detected, indicating a sufficient stiffness and strength of the AM basic body.

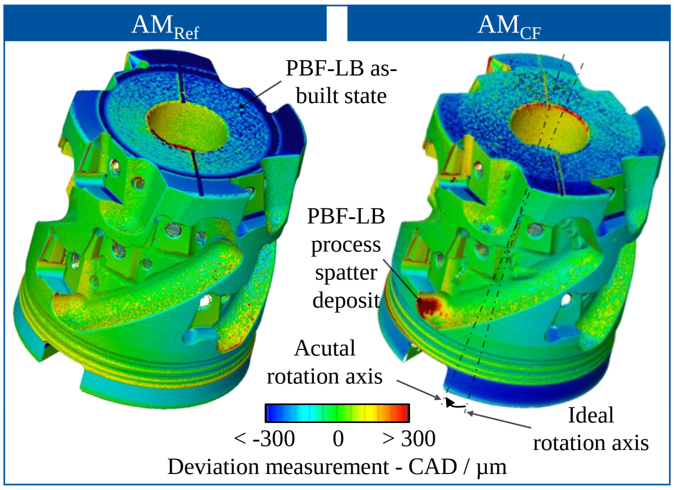

Fig. 6. Geometrical accuracy of AM tools measured by optical 3D scan

The operational tool AM_{CF} and exemplary microscopic images of the outlet nozzles are presented in Fig. 7. The PBF-LB process produced high surface roughness, which can also affect the free jet formation. Therefore, the cross-section of the nozzle outlets were designed oversized between 15 and

20 % (depending on the cross-sectional area) in the CAD model according to the guidelines developed in [14] to maintain the required cross-sectional area in reality.

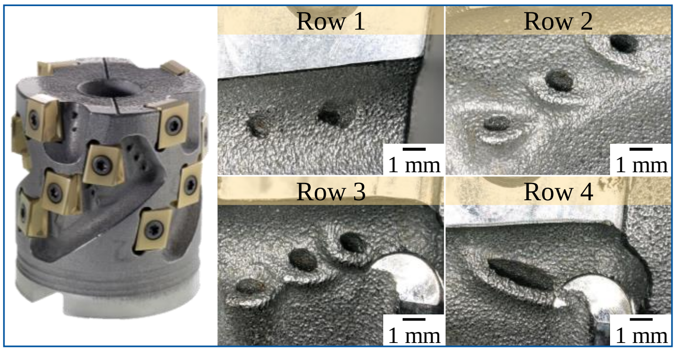

Fig. 7. Insert-equipped additively manufactured tool AM_{CF} and microscopic images of each row

4. Machining experiments

4.1. Experimental setup and workpiece material

The machining experiments were conducted on a machine tool MAG H5000 at Premium AEROTEC in Varel, Germany as shown in Fig. 8. The machine was equipped with a Knoll KF900 high-pressure unit. Blaser B-Cool 755 (8 %) cutting fluid was used with a pump pressure of p = 100 bar. A machine with a maximum available torque of 1500 Nm is used in similar conditions when manufacturing structural components made from Ti-6Al-4V (milling operation with indexable tool with 47 % share of total main time) [20].

Fig. 8. Experimental setup on a machine tool MAG H5000 at Premium AEROTEC Varel, Germany

For the experiments, β-annealed Ti-6Al-4V was machined with the cutting parameters given in Table 3 (feed travel path per shoulder $l_f = 500$ mm). For the tool life test, a part slot milling operation was used. For further testing with increased mechanical load, a full slot milling operation was applied. The three tools introduced in Table 2 were tested during the machining experiments. Cutting inserts of the type Walter Tools LNHU130608R-L55T WSP45G with a $TiAlN+Al_2O_3+(ZrN)$ coating were used. Each tool was equipped with a new batch of 16 unused inserts. All tools covered a total feed travel path of $l_f = 7$ m (cutting time $t_c = 77$ min).

Table 3. Cutting parameters applied during the experiments

	Part slot	Full slot
Depth of cut a_p / mm	40	20
Width of cut a_e / mm	10	63
Feed per tooth f_z / mm	0.1	0.1
Cutting speed v_c / m/min	45	45
Material removal rate Q / cm^3/min	36.4	114.6

4.2. Performance evaluation

In a first step, the AM tool with adapted fluid supply AM_{CF} was tested in full slot milling. The AM basic body withstood the mechanical torsion load and bending force without any detectable incident. No problems regarding chip evacuation or chip jamming due to the rough surface within the chip spaces could be observed. The chips displayed significant curl with the chip volume being smaller than the chip space.

In a second step, the three tools were compared in part slot milling, analyzing tool wear, torque and chip form. The tool wear state was regularly inspected with a Leica DMS300 digital light microscope during the experiments. For a detailed analysis of the tool wear state, after the defined feed travel path, a Keyence VHX900F digital light microscope was used. Explanatory images can be found in Fig. 9. The tool wear was homogenous along the cutting edge with irregular chipping phenomena on the rake face only. The continuous tool wear on the flank face indicates an adequate mechanical tool load [21]. As can be identified from SEM (Scanning electron microscope) images shown in Fig. 10, abrasion was the main wear mechanism, with slight workpiece material adhesions visible on the flank face. First signs of notch wear were visible especially for tool *Ref* in the fourth row of inserts.

The measurement results of the width of flank wear land VB are displayed in Fig. 9. The mean value was calculated by two measurement lines per image of all four inserts per row. On average, the tool wear of the AM_{CF} tool was 27 % lower compared to the reference *Ref*. The biggest improvements appeared in row four (-39 %) due to the reduced notch wear and in row one (-26 %). The AM tool standard fluid supply AM_{Ref} exhibited slightly lower VB values compared to the conventional tool *Ref*. As the cutting fluid supply was similar for both tools and the run-out values lower for *Ref*, this difference might be explained by statistical uncertainty (standard deviation indicated in Fig. 9).

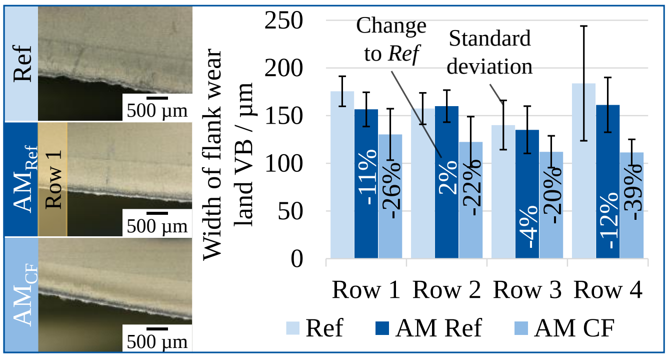

Fig. 9. Tool wear on flank face after a feed travel path of l_f = 7 m

The SEM images shown in Fig. 10 highlight the differences in tool wear between the tools *Ref* and *AM$_{CF}$*. EDX (Energy-dispersive X-ray spectroscopy) analyses indicated black-appearing oxidation on the flank and rake face, which might result from evaporated cutting fluid. The area of oxidation was more pronounced for *Ref*. As the cutting edge is subjected to improved cooling, the heated area is reduced and evaporation only occurs along an area closer to the heat-acquiring cutting edge.

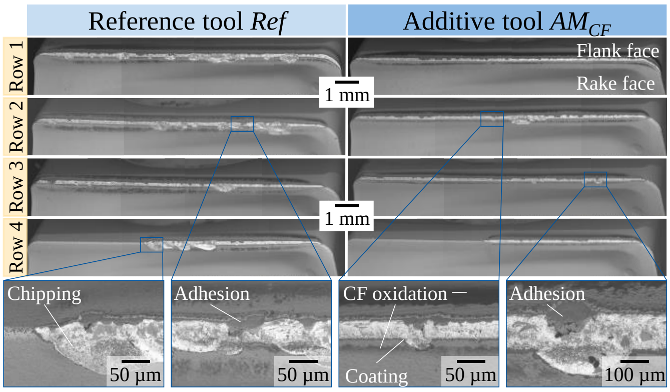

Fig. 10. SEM images of worn cutting inserts of each row for tools *Ref* and *AM$_{CF}$* after a feed travel path of l_f = 7 m

Black appearing friction or abrasion marks were visible on the rake face. Explanatory images for the second and third row are given in Fig. 11. For *Ref* and *AM$_{Ref}$*, long marks were visible in rows 2, 3 and 4. These result from the emerging chip sliding over the rake face. The characteristic marks almost disappeared totally for *AM$_{CF}$*. The chip rear side is impacted by the fluid jet and lifted from the rake face, resulting in less contact to the insert surface. The chip forms analyzed support this finding, see Fig. 14.

For *AM$_{CF}$*, fine black lines are apparent in large quantities on the rake face especially row 2 and 3. An EDX analysis revealed workpiece material adhesion on the coated surface (see Fig. 11). As the contact areas between chip and rake face due to the emerging chip flow are reduced with an improved CF supply, the adhesions must result due to other reasons. One possible explanation might be the fluid flow in the chip space. After the chip is formed, it is not directly ejected from the chip space but drawn back towards the rake face due to a vortical flow field. Further CFD analyses will be performed in the future for a better understanding of the CF free jet flow characteristics.

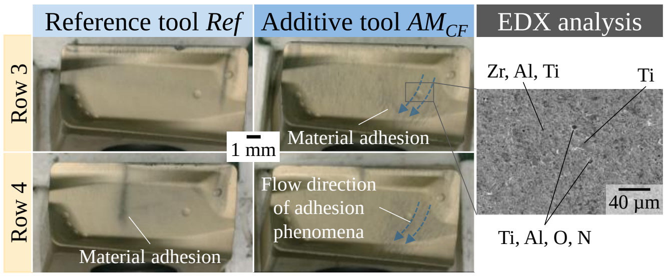

Fig. 11. Tool wear on rake face for tools *Ref* and *AM$_{CF}$* after a feed travel path of l_f = 7 m

Throughout the tool life tests, the torque M was indirectly calculated from measured machine internal signals. As this system is a user-specific development by Premium AEROTEC, no further information can be given. The analysis showed similar torque amplitude and trajectories for all tools as shown in Fig. 12. These results are in accordance with findings obtained by Lakner [2]. The adapted cutting fluid supply with a pressure of p = 100 bar does not significantly change the contact conditions in the milling process. Therefore, cutting force and torque are not significantly different between the tools. The signal did not show any sign of different damping behavior of the tools which is in accordance to findings presented by Kelliger et al. [15].

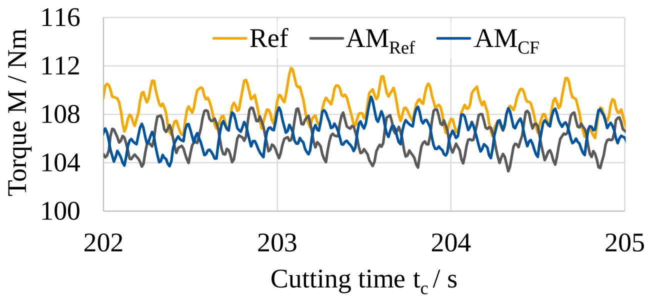

Fig. 12. Explanatory signal from indirect torque measurement at Premium AEROTEC ($l_f \approx 1$ m)

The contact length l_c defines the contact area between chip and rake face [22]. Due to the focused high-pressure CF jet on the rake face in the gap between emerging chip and rake face, the contact length is reduced. Fig. 13 shows the mean l_c-values for all inserts of one row measured by optical light microscopy. With an adapted and focused CF supply, the contact length was reduced by approx. 13 % for *AM$_{CF}$* compared to *Ref*. Even though the local stresses at the cutting edge are increased due to the lower surface area with similar cutting force, in the scope of the investigations this did not have a negative impact on the tool life due to mechanical overload. The positive effect of an improved cooling and lubrication action closer to the highly thermo-mechanical stressed region seem to be the dominant factor.

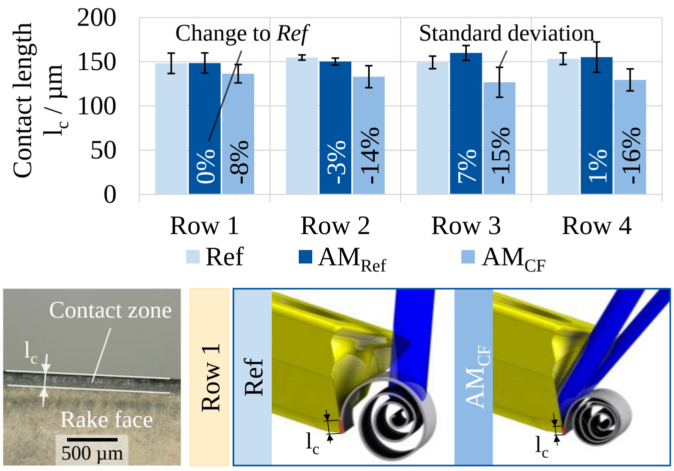

Fig. 13. Contact length on rake face after a feed travel path of l_f = 7 m and CF impact point on emerging chip for different fluid supplies

The mechanical action of the concentrated fluid jet, visible in the reduced contact area, also affected the chip formation as schematically shown in Fig. 13. The average sectional diameter (three measured chips each) presented in Fig. 14 was reduced by approx. 25 % for tool AM_{CF}. A focused CF supply which impacts the chip rear side right after the chip emerges can help to improve chip evacuation due to smaller chips, leaving the possibility for a redesign of the chip space or the introduction of an additional insert [2]. Thus, process reliability and productivity can be improved.

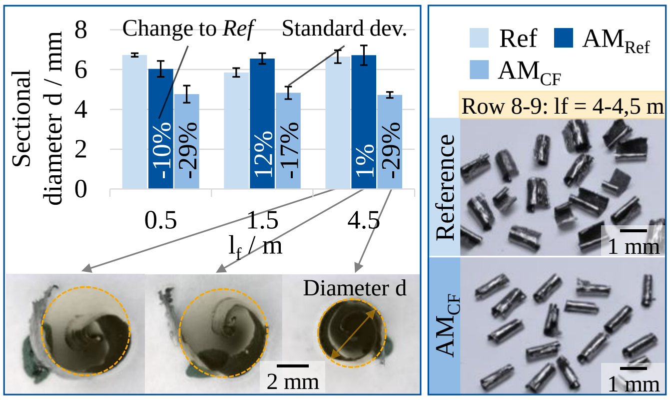

Fig. 14. Chip form and sectional diameter at different feed travel path

5. Conclusion and outlook

In the work presented, a 16-edged, four-row indexable helical milling tool was provided with an adapted internal cutting fluid supply. The tool was PBF-LB additively manufactured with a low-alloyed case hardening steel, post-processed and employed in heavy duty machining experiments during roughing of aerospace-alloy Ti-6Al-4V in an industrial environment. The design of the cutting fluid supply considered the geometrical freedom of design offered by AM techniques. The redesign of channels and outlet nozzles aimed to increase the overall efficiency of the high-pressure cutting fluid supply by reducing pressure losses, increasing volume flow and focusing the cutting fluid free jet to the areas where high cooling and lubrication rates are most needed. A conventionally manufactured reference tool was compared to an AM tool with reference fluid supply as well as to an AM tool with adapted, redesigned fluid supply. The following conclusions are presented:

- The AM tools withstood the applied load in full slot as well as in part slot milling and did not show any sign of plastic deformation.
- The overall wear-affected area of the cutting edge on flank and rake face was smaller for the AM tool with the adapted fluid supply. The tool wear on the flank face was reduced by an average of 27 %, appearing less severe and irregular. Less chipping phenomena occurred on the rake face.
- Fine material adhesion became visible on the rake face for the adapted fluid supply. These might result from the fluid flow characteristics within the chip space, swirling the chip back on the insert surface.
- The contact area between rake face and chip was reduced in length by approx. 13 % due to the mechanical action of the cutting fluid free jet.
- The chip volume was reduced by approx. 25 % due to the narrow rolling of the chip that was supported by the mechanical action of the fluid jet.

The results highlight the potential and the operational readiness of PBF-LB manufactured indexable milling tools for demanding applications. In future work, the acting mechanisms of a focused cutting fluid supply in interrupted cutting need to be further investigated. Especially the influence of a focused CF free jet on the temperature development at the cutting edge needs to be better understood. Furthermore, the fluid flow characteristics in the chip space will be investigated by means of CFD simulation to define improved design guidelines for an adapted CF supply in AM milling tools.

Acknowledgements

The IGF-research project 21049 N (Acronym: “TaCoMA”) of the Forschungsgemeinschaft Werkzeuge und Werkstoffe e.V. (FGW) is funded by the AiF within the program to promote joint industrial research (IGF) by the Federal Ministry for Economic Affairs and Climate Action, following a decision of the German Bundestag.

The authors would like to thank the companies Walter AG and Premium AEROTEC GmbH for the support and provision of tools, material and machine. The PBF-LB manufactured tools within the research project were provided by the Fraunhofer Institute for Laser Technology (ILT) in Aachen, Germany.

References

[1] Bermingham, M.J., Palanisamy, S., Morr, D., Andrews, R., and Dargusch, M.S. “Advantages of milling and drilling Ti-6Al-4V components with high-pressure coolant.” *The International Journal of Advanced Manufacturing Technology* Vol. 72 1-4 (2014): pp. 77–88. DOI 10.1007/s00170-014-5666-1.

[2] Lakner, T. “High-pressure cutting fluid supply in milling.” Dissertation. RWTH Aachen University, Aachen (2021).

[3] Denkena, B., Abele, E., Brecher, C., Dittrich, M.-A., Kara, S., and Mori, M. “Energy efficient machine tools.” *CIRP Annals* Vol. 69 No. 2 (2020): pp. 646–667. DOI 10.1016/j.cirp.2020.05.008.

[4] Klocke, F., Döbbeler, B., and Lakner, T. “Influence of cooling nozzle orientation on the machinability of TiAl6V4 and 42CrMo4+QT in rough milling.” *Procedia CIRP* Vol. 77 (2018): pp. 66–69. DOI 10.1016/j.procir.2018.08.217.

[5] Diegel, O., Nordin, A., and Motte, D. *A Practical Guide to Design for Additive Manufacturing*. Springer, Singapore (2019).

[6] Scherer, T. “Beanspruchungs- und fertigungsgerechte Gestaltung additiv gefertigter Zerspanwerkzeuge.” Dissertation. TU Darmstadt, Darmstadt (2020).

[7] Vogel, F.A.M., Berger, S., Özkaya, E., and Biermann, D. “Vibration Suppression in Turning TiAl6V4 Using Additively Manufactured Tool Holders with Specially Structured, Particle Filled Hollow Elements.” *Procedia Manufacturing* Vol. 40 (2019): pp. 32–37. DOI 10.1016/j.promfg.2020.02.007.

[8] Heep, T. “Funktionsintegriertes Drehwerkzeug zur Effizienzsteigerung kryogener Kohlendioxidkühlung.” Dissertation. TU Darmstadt, Darmstadt (2019).

[9] Mapal Dr. Kress KG. “Lasersintern erweitert Fertigungsmöglichkeiten von Präzisionswerkzeugen.” *Diamond Business* (2017).

[10] Karl-Heinz Arnold GmbH. “Florett statt Bazooka.” *WB Werkstatt + Betrieb No.* 3 (2021): pp. 24–26.

[11] Stokes, N. “Lightweight CoroMill® 390 produced using additive manufacturing reduces vibration in long-overhang milling: Sandvik Coromant.” (2019). last accessed May 25, 2023. URL https://www.sandvik.coromant.com/en-gb/press/lightweight-coromill-390-additive-manufacturing.

[12] Lakner, T., Bergs, T., and Döbbeler, B. “Additively manufactured milling tool with focused cutting fluid supply.” *Procedia CIRP* Vol. 81 (2019): pp. 464–469. DOI 10.1016/j.procir.2019.03.118.

[13] Lakner, T., Bergs, T., and Schraknepper, D. “A Novel Test Bench to Investigate the Effects of the Tool Rotation on Cutting Fluid Jets to Improve the Tool Design via Additive Manufacturing.” *Procedia CIRP* Vol. 91 (2020): pp. 9–14. DOI 10.1016/j.procir.2020.02.144.

[14] Kelliger, T., Liu, H., Schraknepper, D., and Bergs, T. “Investigations on the Impact of Additively Manufactured Coolant Channels and Outlet Nozzles on Free Jet and Jet Forces in High-Pressure Cutting Fluid Supply.” *SSRN Electronic Journal* (2021). DOI 10.2139/ssrn.3936402.

[15] Kelliger, T., Meurer, M., and Bergs, T. “Perfomance Evaluation in Additively Manufactured and Hybrid Indexable Milling Tools in Machining of AISI4140+QT and Ti-6Al-4V.” *Proceedings of ASME Turbo Expo 2023 - Turbomachinery Technical Conference and Exposition* (2023): (published soon).

[16] Kelliger, T. and Saewe, J. *Additively manufactured cutting tools with focused cutting fluid supply*, Aachen Conference on Machining 2022, Aachen (2022).

[17] Deutsches Institut für Normung (2021). “DIN 8030: Fräsköpfe für Wendeschneidplatten: Face milling cutters for indexable inserts.” Deutsche Norm.

[18] Deutsche Edelstahlwerke Specialty Steel GmbH & Co. KG. “Datasheet - Bainidur AM.” (2020).

[19] Bartels, D., Novotny, T., Mohr, A., van Soest, F., Hentschel, O., Merklein, C., and Schmidt, M. “PBF-LB/M of Low-Alloyed Steels: Bainite-like Microstructures despite High Cooling Rates.” *Materials (Basel, Switzerland)* Vol. 15 No. 17 (2022). DOI 10.3390/ma15176171.

[20] Heuwinkel, M., Möller, C., and Dege, J.Hendrik. *Entwicklung eines tangentialen Walzenstirnfräskonzeptes für Titanstrukturbauteile*, Hanser Tagungen "Schwer zerspanbare Werkstoffe in der industriellen Praxis" (2021).

[21] Klocke, F. *Manufacturing Processes 1: Cutting*. Springer, Berlin, Heidelberg (2011).

[22] Iqbal, S.A., Mativenga, P.T., and Sheikh, M.A. “Contact length prediction: mathematical models and effect of friction schemes on FEM simulation for conventional to HSM of AISI 1045 steel.” *Int. J. Machining and Machinability of Materials* Vol. 3, Nos. 1/2 (2008).